NÖHÜ Müh. Bilim. Derg. / NOHU J. Eng. Sci., 2023; 12(4), 1481-1491

Niğde Ömer Halisdemir Üniversitesi Mühendislik Bilimleri Dergisi
Niğde Ömer Halisdemir University Journal of Engineering Sciences

Araştırma makalesi / Research article

www.dergipark.org.tr/tr/pub/ngumuh / www.dergipark.org.tr/en/pub/ngumuh

Optimal sizing of grid-connected hybrid energy systems for electric vehicle charging stations considering charging demand periods and economic parameters

Elektrikli araç şarj istasyonları için şebekeye bağlı hibrit yenilenebilir enerji sistemlerinin şarj talep dönemleri ve ekonomik parametreler göz önünde bulundurularak optimum boyutlandırılması

Alpaslan Demirci*

Department of Electrical Engineering, Yildiz Technical University, İstanbul, Türkiye

Abstract

The development of electric vehicle (EV) technologies and the spread of EVs have made expanding charging infrastructure increasingly critical. However, unplanned sizing of EV charging stations will have adverse technical, economic, and environmental impacts, especially on grid reliability and energy costs. This study performs a techno-economic evaluation of a solar PV-based hybrid power system considering variations in EV charging demand profiles and economic parameters. The results show that variations in demand profile and economic parameters significantly influence investment decisions. Higher inflation was most effective on peak evening demand profiles, increasing the levelized cost of energy by up to 2.2 times. Self-sufficiency can increase to 57% under grid sales constraints in the midday peak scenario. Moreover, at maximum installed PV capacity, the self-consumption rate (SCR) is 12% higher than in the evening peak, and curtailment is reduced by up to 4.5%. The results will expand the use of renewable energy with less grid dependency and faster achievement of zero carbon emission targets.

Keywords: Electric vehicle, Electric vehicle charging station, Energy storage systems, Hybrid power system, Optimization, Renewable energy source.

Özet

Elektrikli araç (EA) teknolojilerinin gelişmesi ve EA'ların yaygınlaşması, şarj altyapısının genişletilmesini giderek daha kritik hale getirmiştir. Plansız EA şarj istasyonu boyutlandırması, özellikle şebeke güvenilirliği ve enerji maliyetleri üzerinde olumsuz teknik, ekonomik ve çevresel etkilere sahip olacaktır. Bu çalışmada, EA şarj talep profilleri ve ekonomik parametrelerdeki değişimleri göz önünde bulundurarak, güneş fotovoltaik tabanlı hibrit güç sisteminin tekno-ekonomik değerlendirmesi yapılmıştır. Sonuçlar, talep profilindeki ve ekonomik parametrelerdeki değişkenliklerin yatırım kararlarını önemli ölçüde etkilediğini göstermektedir. Yüksek enflasyon en çok pik gece şarj talebi profillerinde etkili olmuş ve seviyelendirilmiş enerji maliyetini 2,2 katına kadar artırmıştır. Şebeke satış kısıtlamaları altında öğlen zirve senaryosunda kendi kendine yeterlilik %57'ye kadar artabilir. Dahası, maksimum fotovoltaik kurulu gücünde öz tüketim oranı akşam zirve senaryosuna göre 12% daha yüksek olmayı başarmış ve faydalanılamayan enerji %4,5'e kadar azalmıştır. Sonuçlar, şebekeye daha az bağımlı yenilenebilir enerji kullanımını yaygınlaştıracak ve sıfır karbon emisyonu hedeflerine daha hızlı ulaşılmasını sağlayacaktır.

Anahtar Kelimeler: Elektrikli araç, elektrikli araç şarj istasyonu, enerji depolama sistemleri, hibrit güç sistemi, optimizasyon, yenilenebilir enerji kaynağı

1 Introduction

As global temperatures reached alarming levels, countries had to turn to new energy alternatives. Moreover, it is necessary to reduce the negative impact of energy-consumption vehicles, especially fossil fuel-dependent cars, on the environment. It promises that by 2050, the share of EVs in the automobile market will reach 81.5%, and the share of renewables in energy production will get 88% with net zero emission commitments set in global partnerships to which countries are a party. The widespread penetration of electric vehicles (EVs) could reduce the role of transportation in environmental pollution. However, the increased energy demand for EVs will increase the peak load capacity of the grid. Therefore, integrating renewable technologies is increasingly important to meet the growing demand for EV charging stations (EVCS) without grid dependency. Analyses of sensitivity and incorporating inflation rates (IR) and discount rates (DR) into financial models are required for optimal diesel generator (DG) allocation. This allows for a more comprehensive assessment of different allocation decisions' economic viability and potential risks. IR can affect the cost of materials and labor required to construct renewable energy facilities. Therefore, as IR increases, project costs may also increase. Higher project costs may affect optimal allocation decisions, making DGs less attractive. IR&DR are linked, and higher DR can affect the cost of borrowing for hybrid power system projects. Higher DR increases the cost of capital and potentially reduces financing options' attractiveness. Therefore, optimal sizing may be affected as projects with higher financing costs become less favorable. On the other

* Corresponding author, e-posta / e-mail: ademirci@yildiz.edu.tr (A. Demirci)
Geliş / Recieved: 02.07.2023 Kabul / Accepted: 17.09.2023 Yayımlanma / Published: 15.10.2023
doi: 10.28948/ngumuh.1321628

hand, IR can affect investment returns for DG projects. Therefore, it is important to consider inflation-adjusted returns when assessing the financial viability of DG projects. Higher IR can reduce real returns. IR can also affect electricity tariffs and revenues from DG systems. If electricity tariffs are not indexed to inflation, the purchasing power of income from DG projects may decline over time. So, IR&DR are critical inputs when conducting discounted cash flow analysis, which is widely used to assess the financial feasibility of DG projects. Higher IR can affect the present value of future cash flows by affecting the DR used in cash flow analysis. These rates can alter the financial attractiveness of DG projects and influence optimal allocation decisions.

Various studies analyze the optimal sizing of HPS and its possible technical, economic, and environmental effects. The energy demand at EVCS, which is almost universal, can be supplied by PV. EVCS optimal installation points are determined by a four-stage analysis that works in harmony with the GIS-based approach to improve system performance [1]. The available PV capacity was determined as 3.1 MW for 100 EV charging points and 11.1 GW across the US [2]. Self-consumption data in five different Chinese cities were improved with a new methodology developed to avoid bicycle charging current limit at public transportation stations and to use PV effectively in different irradiances [3]. Thanks to the optimization approach developed, cumulative CO_2 was reduced by up to 15%, while EV charging demand was met by over 93% [4]. The multi-objective optimization model reduced COE to 0.046 $/kWh and CO_2 to 472.4 g [5]. In another study, where supply-demand uncertainties were removed with Monte Carlo and EV charging was determined with the Erlang B queuing model, the annual energy cost purchased from the grid was reduced by 74.2%. In comparison, the revenue from energy sales increased by 19.86% [6]. The system's operating costs were reduced by 42.8% using an economic linearized stochastic programming strategy that included the electricity tariff [7]. In building communities with EVCS, by removing biomass generators from the optimal configuration, COE was decreased by 17.5%, while energy supply was increased by 8.33% [8]. In another study, optimizing using ABC&PSO improved RF by up to 87%, while COE and LPSP were reduced to $0.038/kWh and 0.19%, respectively [9].

Although the optimization methods focus on optimal sizing, the network needs strengthening due to increasing demand and capacity constraints. Time of Use (TOU) is a pricing structure used primarily in the energy and utility industries to charge customers based on the hours they use electricity or other utilities. TOU pricing aims to create a more efficient and sustainable electricity system by aligning consumer behavior with daily energy supply and demand fluctuations [10]. This encourages consumers to use electricity while it is cheaper, which can ultimately lead to cost savings and a more reliable grid. However, its success depends on consumer education and their ability to change their routines to take advantage of lower off-peak prices. TOU pricing can be complex for consumers to understand and manage. Consumers may face higher initial bills if they do not change their habits to take advantage of off-peak pricing [11]. Evidence shows that small to medium-sized commercial customers are willing to reduce their peak energy consumption due to TOU pricing [12]. The energy management strategy developed based on TOU considers the benefits of network operators and users, reduces costs, and shortens the payback period to 5.17 years [13]. In recent years, TOU and real-time pricing have received increasing attention, especially with the advent of the smart grid, which allows the implementation of TOU [14–16].

Grid operators must use each generating and consuming system for different grid services. By playing an active role in the energy market, power quality issues in the grid can be addressed, while the potential of the smart grid can be enhanced with more options for customers. The performance of the solar EVCS is evaluated using accurate load data and meteorological measurements, considering the seasonal effect of PV generation. The PV generation size and EV charging connection time were varied and analyzed under different scenarios, and it was observed that level-2 charging does not cause voltage instability. It was also emphasized that it could reduce the probability of under-voltage problems, transformer overload, and losses due to PV generation and EV charging demand [17]. It has been determined that the carbon footprint of solar EVCS with energy storage systems (ESS) can be reduced by up to 15% with an environmentally optimized design [4]. These studies mostly optimized system sizing by considering variables such as EV charging, PV capacity, and solar irradiance variations. However, the uncertainty associated with EV charging and the potential for economic parameters such as IR&DR to fluctuate has not been simultaneously analyzed. This study explores the potential for integrating renewable energy system (RES) into EVCS by considering EV charging demand periods and financial parameter variability. The original contributions of this paper are as follows:

- Techno-economic evaluation of a grid-connected hybrid power system for electric vehicle charging stations has been performed.
- Investment decisions are significantly influenced by variations in the demand profile and economic parameters.
- The performance of the hybrid energy system is examined in detail through sensitivity analysis.
- The potential for direct energy transfer from PV to load and the techno-economic impacts are analyzed according to the variation in the demand period.
- The levelized energy cost increases by up to 55% in the evening peak, depending on the variation in economic parameters.

This paper investigates the potential of retrofitting EVCSs with solar PV, considering variations in energy demand times for EVCS and economic parameters such as IR&DR.

2 Material and method

2.1 Location and climatic data

Antalya city in Türkiye is 36° 53.8' latitude and 30° 42.8' longitude. Figure 1 shows Antalya's average solar radiation, temperature, and clearness index data [18].

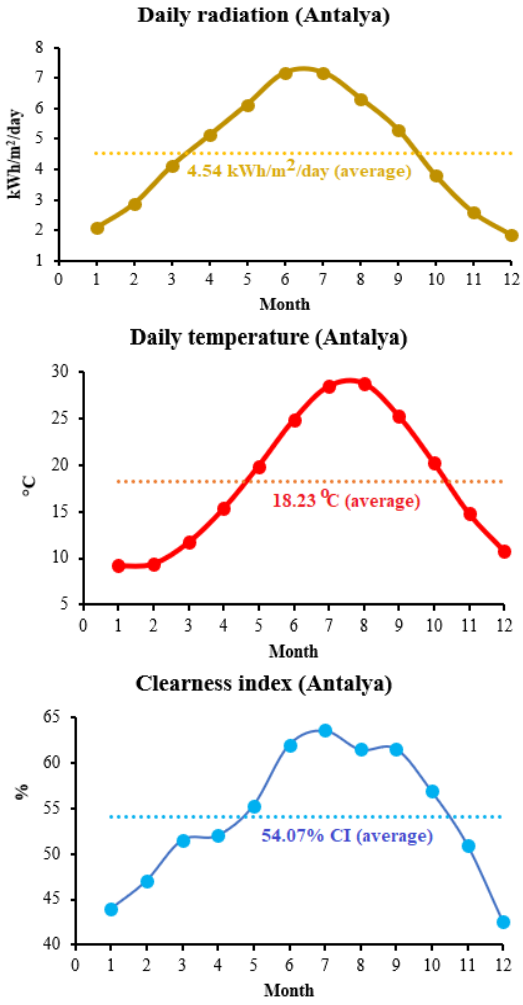

Figure 1. Solar radiation, temperature, and clearness index (CI) data in Antalya.

Average solar radiation data for each month is obtained from the National Aeronautics and Space Administration (NASA) using the software database. The data is Antalya's average daily radiation, average temperature, and average clearness index is 4.54 kWh/m^2/day, 18.23°C, and 54.07%.

2.2 Solar photovoltaic panel

The solar photovoltaic panel is the main component of HPS. The PV array performance varies depending on solar radiation, panel temperature, derivative factor (DF), and panel efficiency. The amount of power produced by the PV array at time t $P_{PV}(t)$ is given in Equation (1), the maximum efficiency formula of PV panels under normal conditions (STC) $\eta_{mp,STC}$ is given in Equation (2), and cell temperature at time t $T_C(t)$ formula of PV array under operating condition is given in Equation (3) [19]. Where Y_{PV} is PV array rated capacity in STC (kW), f_{PV} is PV derating factor (%), $G_T(t)$ is solar radiation at time t (kW/m^2), $G_{T,STC}$ is measurement of incident radiation at STC (1 kW/m^2), α_P is temperature coefficient of power (0.1%/^{0}C), $T_a(t)$ is ambient temperature at time t (^{0}C), T_{NOCT} is normal operation cell temperature (^{0}C), and A_{PV} is area of the PV panel (m^2) [20].

$$P_{PV}(t) = \frac{Y_{PV}.f_{PV}.G_T(t).\left[1+\alpha_P.\left(T_C - T_{C,STC}\right)\right]}{G_{T,STC}} \quad (1)$$

$$\eta_{mp,STC} = \frac{Y_{PV}}{A_{PV}.G_{T,STC}} \quad (2)$$

$$T_C(t) = T_a(t) + \frac{G_T(t).(T_{NOCT} - 20)}{800} \quad (3)$$

2.3 Converter (inverter and rectifier)

Converters are required for energy flow between DC and AC systems in HPS. It consists of a converter, rectifiers, and an inverter. Proper sizing of the converter power is critical in correctly sizing the HPS model. A small converter can curtail a considerable amount of energy. The power output formula of the inverter at time t $P_{inv}(t)$ is shown in Equation (4), and the power output formula of the rectifier at time t $P_{rec}(t)$ is seen in Equation (5) [21]. Where $P_{DC}(t)$ is DC power input at time t (kW), $P_{AC}(t)$ is AC power input at time t (kW), η_{inv} is inverter efficiency (%), and η_{rec} is rectifier efficiency (%).

$$P_{inv}(t) = \eta_{inv}.P_{DC}(t) \quad (4)$$

$$P_{rec}(t) = \eta_{rec}.P_{AC}(t) \quad (5)$$

2.4 EVCS and peak time ranges

The time horizon for the charging of each j EV of type e (hour) ($\tau_{e,j}$) is given in Equation (6), the charge power of each j EV of type e at time t (kW) ($P_{EV(e,j)}(t)$) in Equation (7), and total EV power at time t (kW) (P_{EV}^t) are given in Equation (8) [22]. Where $st_{e,j}$ is starting charge time of j EV of type e (hour), ER_e is average required energy for EV type e (kWh), $P_{EV(max)}$ is maximum charging power in slow mode for EV type e (kW), $P_{EV(j,t)}$ is charging power of j EV of type e at time t (kW), N_{EV} is the number of EV, j is EV user index, t is time index (hour), and e is EV type ($e = 1$ cars).

$$\tau_{e,j} = \left[st_{e,j} + \frac{ER_e}{P_{EV(max)}}\right] \quad (6)$$

$$P_{EV(e,j)}(t) = \begin{cases} P_{EV(max)} & if\ t \in \tau_{e,j} \\ 0 & if\ t \notin \tau_{e,j} \end{cases} \quad (7)$$

$$P_{EV}^t = \sum_{j=1}^{N_{EV}} P_{EV(e,j)}(t) \quad (8)$$

Table 1 shows the different EVCS peak times and daily energy demands. This study created EVCS load profiles considering three different peak time periods. The average daily demand of EVCSs is 2500 kWh/day. In addition, the peak charging demand times are between 07.00-09.00 in the morning in EVCS1, 11.00-13.00 in EVCS2, and 17.00-19.00 in EVCS3.

Table 1. EVCS peak times and daily energy demands

	EVCS Types		
	EVCS1	*EVCS2*	*EVCS3*
Peak Time Range	07.00-09.00 Morning Peak	11.00-13.00 Midday Peak	17.00-19.00 Evening Peak
Energy Demand	2479 kWh/day	2505 kWh/day	2496 kWh/day

2.5 *Energy storage system*

Energy storage system (ESS) stores the excess energy produced, supplies energy to the HPS that needs energy, and provides a constant voltage in case of incompatibility between power generation and consumption. Thus, they establish the balance between the energy produced and the load demand. The capacity value of the ESS (C_{ESS}) is given in Equation (9). Where E_{load} is average daily load energy (Ah), D_{ESS} is number of days energized by ESS, DOD_{max} is battery maximum discharge depth [%], η_{ESS} is ESS efficiency [%], and η_{inv} is inverter efficiency [%] [23, 24].

$$C_{ESS} = \frac{E_{load} \cdot D_{ESS}}{1000 \cdot DOD_{max} \cdot \eta_{ESS} \cdot \eta_{inv}} \ [kWh] \qquad (9)$$

2.6 *HPS models and cost prices*

Hybrid energy systems are defined as systems that use multiple energy sources such as solar and wind, solar and diesel generators, wind and diesel generators, or solar, wind, and diesel generator systems to power the electrical load and can integrate with the electricity grid [25]. Figure 2 shows the HPS model. Capital, replacement, and operation & maintenance (O&M) costs of HPS components are given in Table 2 [26]. The project lifetime of the HPS is 20 years.

Table 2. EVCS model component prices

	HPS Model Components		
	PV	*ESS*	*Converter*
Capital Cost	1000 $/kW	300 $/kWh	300 $/kW
Replacement Cost	900 $/kW	250 $/kWh	300 $/kW
O&M Cost	10 $/kW/yr	2 $/kWh/yr	0.02 $/kW/yr

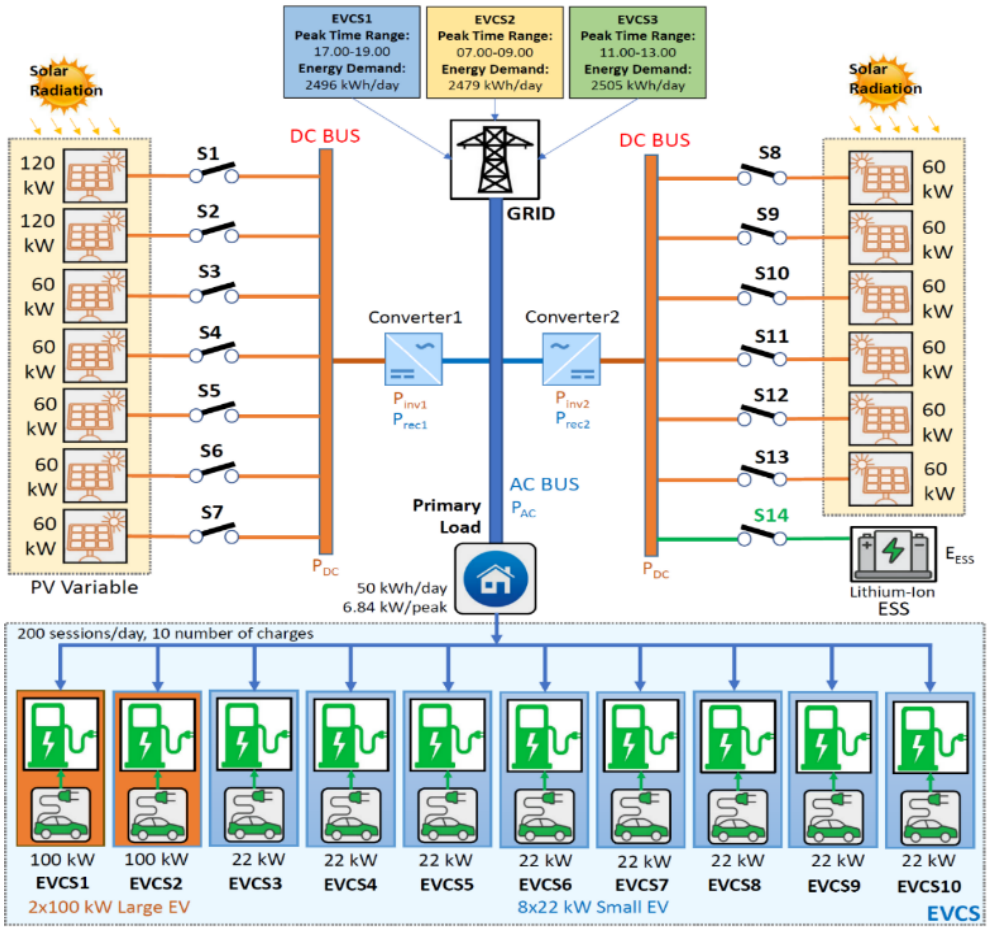

Figure 2. HPS models.

2.7 Grid tariffs and prices

The three-tariff system has been considered in energy purchase and sale, and the purchase-sale cost values of this three-tariff are given in Table 3 [27].

Table 3. Grid price tariffs

Grid Properties		Time Range	Grid Price ($/kWh)
Grid Purchases (TOU)	*Flat Tariff*	06.00-17.00	0.100
	Peak Tariff	17.00-22.00	0.160
	Valley Tariff	22.00-06.00	0.056
Grid Sales		24 hours	0.051

2.8 Economic parameters

The net present cost (NPC) of the system is obtained by subtracting the present value of all costs over the project's life from the present value of all income earned during the project's lifespan. It includes capital cost, replacement cost, O&M cost, grid purchases, and emission cost penalties. HOMER software calculates the NPC value by summing the discounted cash flows at the end of each year. The annual cost is multiplied by the NPC value by the capital recovery factor. NPC ($) at the end of the project lifespan is given in Equation (10), capital recovery factor ($CRF(i,N)$) in Equation (11), and annual real DR (%) (i) in Equation (12) [28]. Where $C_{ann,tot}$ is total annualized cost ($/yr), N is project lifetime (year), n is number of years, i' is nominal DR (%), and f is expected IR (%).

$$NPC = \frac{C_{ann,tot}}{CRF(i,N)} \quad [\$] \tag{10}$$

$$CRF(i,N) = \frac{i\,.\,(1+i)^n}{i\,.\,(1+i)-1} \tag{11}$$

$$i = \frac{i'-f}{1+f} \tag{12}$$

The average cost per kWh of useful energy produced by the HPS represents the levelized cost of energy ($/kWh). It is a suitable metric for comparing HPSs. Equation (13) shows the formula for the COE [29]. Where E_{served} is total electrical load served (kWh/yr).

$$COE = \frac{C_{ann,tot}}{E_{served}} \quad [\$/kWh] \tag{13}$$

Renewable fraction (RF) is a fraction display that shows the rate at which the total annual energy power generation from RES is transferred to the load. The ratio of RES to the loads in the system is managed in this fraction notation. Equation (14) represents the RF [30, 31].

$$RF = 1 - \frac{E_{nonren}}{E_{served}} \quad [\%] \tag{14}$$

The self-consumption rate (SCR) is the ratio between the total PV energy directly transferred to the load ($\sum E_{PV}^{cons}$), and the total PV energy ($\sum E_{PV}^{gen}$), shown in Equation (15) [32]. The ratio between the total RES generation directly transferred to the load and the annual total load demand ($\sum E_{LOAD}$) gives the self-supply rate (SSR). For the SSR to increase, the share of PV should increase according to the load demand. Equation (16) shows the formula for the self-supply ratio [33]. Equation (17) shows the objective function (f) of HPS. The function aims to determine the HPS that minimizes the NPC value.

$$SCR = \frac{\sum E_{PV}^{cons}}{\sum E_{PV}^{gen}} \quad [\%] \tag{15}$$

$$SSR = \frac{\sum E_{PV}^{cons}}{\sum E_{LOAD}} \quad [\%] \tag{16}$$

$$f = \min\left(\sum_{n=1}^{N} NPC\right) \tag{17}$$

Table 4 shows HPS scenarios [34]. HPS scenarios have been created for three different IR&DR parameters. The grid energy sales constraint is considered in the analyses. Also, the maximum PV installed capacity is set at 900kW, considering the limited installed area in EVCSs [35]. The performance of each scenario is evaluated by considering the self-consumption rate, self-sufficiency rate, excess energy, and energy cost parameters.

Table 4. HPS scenarios

Parameters	Case 1	Case 2	Case 3
Inflation rate (IR)	1.30%	7.40%	14.0%
Discount rate (DR)	4.30%	8.49%	23.3%
Grid sale constraint	with GSC, without GSC		
PV capacity	0-120-240-300-360-420-480-540-600-660-720-780-840-900 kW		

3 Optimization results

Prosumers' investment decisions are significantly affected by IR&DR. This section determines the optimal PV capacities according to demand profiles with different peak times for IR&DR. Moreover, the impact of increased PV capacity on technical, economic, and environmental outcomes is assessed. Figure 3 shows that, regardless of the peak time of the load, the optimal PV capacity increases with the increase in IR&DR. It can also be said that SCR decreases and SSR and EE increase with increasing PV capacity in each profile. At optimum PV capacities and highest IR (Case 3), SCR and SSR decrease to 45% and 43%, while EE increases to 33.6% during the morning peak. Increasing PV capacity reduces SCR to 34%, 40%, and 28% in the morning, midday, and evening peak scenarios. So,

SCR is 12% lower in the evening peak than in the midday scenario. In addition, the curtailment energy due to load mismatch is 4.5% higher.

On the other hand, SSR increased to 57% in the midday peak scenarios but could only increase to 48% and 40% in the morning and evening peak, depending on the PV capacity increases. The COE increases with each peak profile for most PV capacities, especially at the lowest inflation. High IR increased the levelized cost of energy by up to 19.2%, 28%, and 20.3% in the morning, midday, and evening peak optimal scenarios, respectively. PV capacities that minimize COE and keep SCR within limits were selected as optimum. Optimal PV capacity increased by 2.5 times during the highest IR compared to under lower IR optimal scenarios for the morning peak. This ratio increased PV capacity by up to 1.8 times and 3 times, respectively, during the midday and evening peak periods in the optimal case for the same situation.

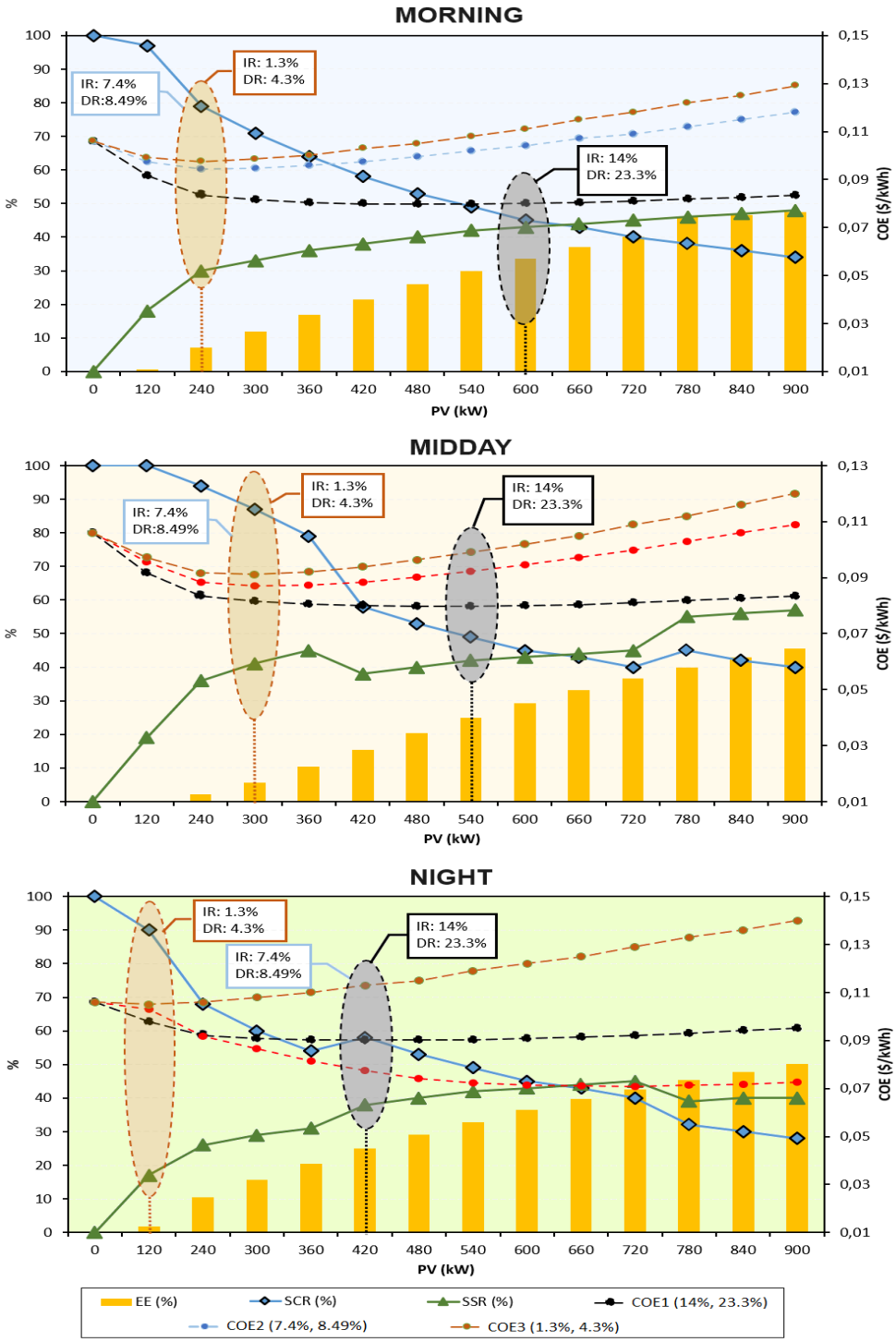

Figure 3. EVCS self-consumption and self-sufficiently change with GSC

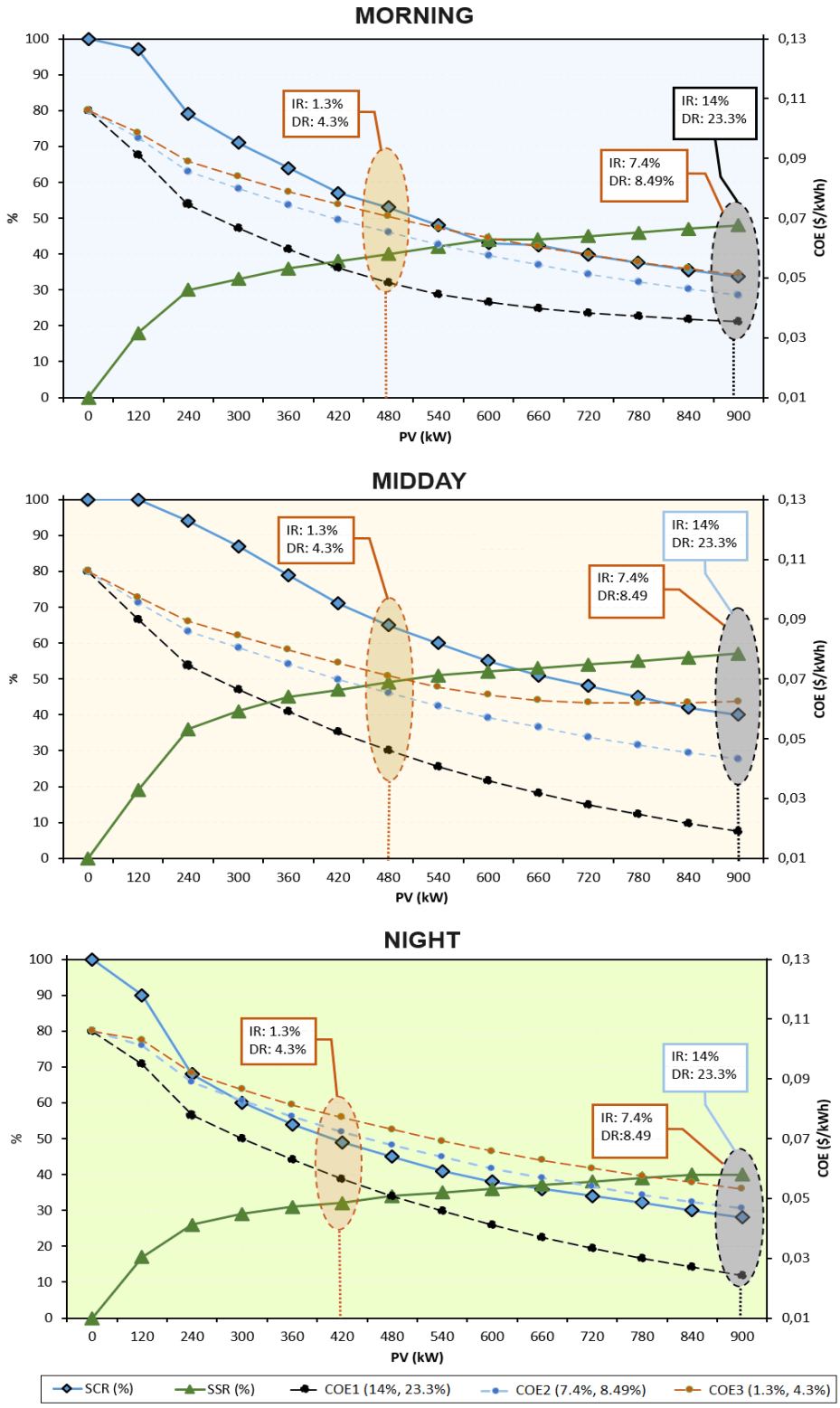

Figure 4. EVCS self-consumption and self-sufficiently change without GSC

Figure 4 shows that EE and COE have decreased with grid sales, and the optimal PV capacity has increased. The absence of over-generated electricity indicates that the sizing strategy is quite important. It can be noted that the revenue received from the sale of electricity to the grid affects the COE and the optimal PV capacity associated with the COE. In this context, SCR and SSR were not much affected by the economic rate and peak time. As IR increased (Case 3), optimal PV capacity increased by 53% for morning and midday peaks and 47% for evening.

The optimal COE decreased by 55.3%, 32.3%, and 28.2% at the morning peak for cases 1, 2, and 3, respectively.

In the case of high IR (Case 3), the SCR decreased by 19.3%, 25%, and 21% in the morning, midday, and evening peak periods, respectively. It should be noted that the SSR increased by 8% in the same situation.

With sales to the grid, SCR was more affected by the evening peak and SSR more by the midday peak. These values will decrease with decreasing inflation. Regardless of the peak time, at high and medium IR (Case 2 and 3), the optimal PV capacity and, thus, the probability of load coverage by the PV is maximized. On the other hand, SSR does not improve the optimal selection of PV capacity at evening peaks and low IR.

4 Conclusion

This paper investigates the potential of retrofitting EVCSs with solar PV, considering variations in energy demand times for EVCS and economic parameters such as IR&DR. Optimization results show that inflation increases COE by up to 28%, depending on different peak charging periods. The increased PV capacity further reduced the SCR by up to 12% for the evening peak. Optimal SSR was 30%, 41%, and 17% for morning, midday, and evening peak, respectively, in the low inflation scenarios. Higher inflation was most affected in the evening peak, increasing the levelized cost of energy by up to 2.2 times. In the optimal scenario with morning peak demand, the SCR increases up to 79% at low inflation but decreases to 45% as inflation increases. In contrast, for the same economic conditions in the evening peaks, the SCR decreases by 32%. The results demonstrate the benefits of EVCS optimization to clean energy management from multiple perspectives, which can support the development of EVCS policies. Future studies should improve the optimal hybrid system sizing methodology considering solar radiation potential, hybrid system installation costs, carbon tax, and incentives.

Conflict of interest

The authors declare that there is no conflict of interest.

Similarity rate (Turnitin): 13%

References

[1] M. Erbaş, M. Kabak, E. Özceylan and C. Çetinkaya, Optimal siting of electric vehicle charging stations: A GIS-based fuzzy Multi-Criteria Decision Analysis. Energy, 163, 1017–1031, 2018. https://doi.org/10.1016/j.energy.2018.08.140.

[2] S. S. Deshmukh and J. M. Pearce, Electric vehicle charging potential from retail parking lot solar photovoltaic awnings. Renewable Energy, 169, 608–617, 2021. https://doi.org/10.1016/j.renene.2021.01.068.

[3] R. Yin and J. He, Design of a photovoltaic electric bike battery-sharing system in public transit stations. Applied Energy, 332, 1-15, 2023. https://doi.org/10.1016/j.apenergy.2022.120505.

[4] L. Bartolucci, S. Cordiner, V. Mulone, M. Santarelli, F. Ortenzi and M. Pasquali, PV assisted electric vehicle charging station considering the integration of stationary first- or second-life battery storage. Journal of Cleaner Production, 383, 1-18, 2023. https://doi.org/10.1016/j.jclepro.2022.135426.

[5] B. Sun, A multi-objective optimization model for fast electric vehicle charging stations with wind, PV power and energy storage. Journal of Cleaner Production, 288, 1-17, 2021. https://doi.org/10.1016/j.jclepro.2020.125564.

[6] J. A. Domínguez-Navarro, R. Dufo-López, J. M. Yusta-Loyo, J. S. Artal-Sevil and J. L. Bernal-Agustín, Design of an electric vehicle fast-charging station with integration of renewable energy and storage systems. International Journal of Electrical Power & Energy Systems, 105, 46–58, 2019. https://doi.org/10.1016/j.ijepes.2018.08.001.

[7] M. Farrokhifar, F. H. Aghdam, A. Alahyari, A. Monavari and A. Safari, Optimal energy management and sizing of renewable energy and battery systems in residential sectors via a stochastic MILP model. Electric Power Systems Research, 187, 1-13, 2020. https://doi.org/10.1016/j.epsr.2020.106483.

[8] S. Kumar and S. Koteswara Rao, Optimum capacity of hybrid renewable energy system suitable for fulfilling yearly load demand for a community building located at Vaddeswaram, Andhra Pradesh. Energy and Buildings, 277, 1-14, 2022. https://doi.org/10.1016/j.enbuild.2022.11257.

[9] S. Singh, P. Chauhan and N. J. Singh, Feasibility of Grid-connected Solar-wind Hybrid System with Electric Vehicle Charging Station. Journal of Modern Power Systems and Clean Energy, 9 (2), 295–306, 2021. https://doi.org/10.35833/MPCE.2019.000081.

[10] S. Amiri-Pebdani, M. Alinaghian and S. Safarzadeh, Time-Of-Use pricing in an energy sustainable supply chain with government interventions: A game theory approach. Energy, 255, 1-18, 2022. https://doi.org/10.1016/j.energy.2022.124380.

[11] S. Panda, S. Mohanty, P.K. Rout, B.K. Sahu, M. Bajaj, H.M. Zawbaa and S. Kamel, Residential Demand Side Management model, optimization and future perspective: A review. Energy Reports, 8, 3727–3766, 2022. https://doi.org/10.1016/j.egyr.2022.02.300.

[12] P. Yang, G. Tang and A. Nehorai, A game-theoretic approach for optimal time-of-use electricity pricing. IEEE Transactions on Power Systems, 28 (2), 884–892, 2013. https://doi.org/10.1109/TPWRS.2012.2207134.

[13] M. Yang, L. Zhang, Z. Zhao and L. Wang, Comprehensive benefits analysis of electric vehicle charging station integrated photovoltaic and energy storage. Journal of Cleaner Production, 302, 1-12, 2021. https://doi.org/10.1016/j.jclepro.2021.126967.

[14] B. Aljafari, P.R. Jeyaraj, A.C. Kathiresan and S.B. Thanikanti, Electric vehicle optimum charging-discharging scheduling with dynamic pricing employing multi agent deep neural network. Computers and Electrical Engineering, 105, 1-16, 2023. https://doi.org/10.1016/j.compeleceng.2022.108555.

[15] K. Victor Sam Moses Babu, K. Satya Surya Vinay and P. Chakraborty, Peer-to-Peer Sharing of Energy

Storage Systems Under Net Metering and Time-of-Use Pricing. IEEE Access, 11, 3118–3128, 2023. https://doi.org/10.1109/ACCESS.2023.3234625.
[16] M.A. Judge, A. Khan, A. Manzoor and H.A. Khattak, Overview of smart grid implementation: Frameworks, impact, performance and challenges. Journal of Energy Storage, 49, 1-18, 2022. https://doi.org/10.1016/j.est.2022.104056.
[17] J.H. Angelim and C. de M. Affonso, Probabilistic assessment of voltage quality on solar-powered electric vehicle charging station. Electric Power Systems Research, 189, 1-10, 2020. https://doi.org/10.1016/j.epsr.2020.106655.
[18] NASA Prediction of Worldwide Energy Resources, 2021. https://data.nasa.gov/Earth-Science/Prediction-Of-Worldwide-Energy-Resources-POWER-/wn3p-qsan (accessed Oct. 08, 2021).
[19] M. Terkes, Z. Ozturk, A. Demirci and S.M. Tercan, Optimal sizing and feasibility analysis of second-life battery energy storage systems for community microgrids considering carbon reduction, Journal of Cleaner Production, 421, 1-14, 2023. https://doi.org/10.1016/j.jclepro.2023.138507.
[20] Homer Energy, 2023. https://www.homerenergy.com/products/pro/docs/latest/index.html (accessed Jul. 10, 2023).
[21] Z. Ozturk and A. Demirci, Optimization of Renewable Energy Hybrid Power Systems Under Different Penetration and Grid Tariffs. Journal of Polytechnic, 26(3), 1267-1275, 2023. https://doi.org/10.2339/politeknik.1246418.
[22] J.M. Clairand, M. Arriaga, C.A. Canizares and C. Alvarez-Bel, Power Generation Planning of Galapagos. Microgrid Considering Electric Vehicles and Induction Stoves. IEEE Transactions on Sustainable Energy, 10 (4), 1916–1926, 2019. https://doi.org/10.1109/TSTE.2018.2876059.
[23] A. Chauhan and R.P. Saini, A review on Integrated Renewable Energy System based power generation for stand-alone applications: Configurations, storage options, sizing methodologies and control. Renewable and Sustainable Energy Reviews, 38, 99-120, 2014. https://doi.org/10.1016/j.rser.2014.05.079.
[24] Z. Ozturk, A. Demirci, S. Tosun and A. Ozturk, Technic and Economic Effects of Changes in the Location of Industrial Facilities in Industrializing Regions on Power Systems, in 2021 13th International Conference on Electrical and Electronics Engineering (ELECO), 11–17, 2021. https://doi.org/10.23919/ELECO54474.2021.9677827.
[25] Y. Yuan, J. Wang, X. Yan, B. Shen and T. Long, A review of multi-energy hybrid power system for ships. Renewable and Sustainable Energy Reviews, 132, 1-15, 2020. https://doi.org/10.1016/j.rser.2020.110081.
[26] I.R.E. Agency, IRENA (2021), Renewable Power Generation Costs in 2020, Abu Dhabi, 2020.
[27] Renewables 2021, Global Status Report, 2021.
[28] A. Demirci, Z. Ozturk and S. M. Tercan, Decision-making between hybrid renewable energy configurations and grid extension in rural areas for different climate zones. Energy, 1–22, 2022. https://doi.org/10.1016/j.energy.2022.125402.
[29] Z. Ozturk, S. Tosun, A. Ozturk and O. Akar, Comparative Evaluation of Stand-Alone Hybrid Power System with Different Energy Storages. Fresenius Environmental Bulletin, 30(9), 10908–10924, 2021.
[30] T. Salameh, M.A. Abdelkareem, A.G. Olabi, E.T. Sayed, M. Al-Chaderchi and H.Rezk, Integrated standalone hybrid solar PV, fuel cell and diesel generator power system for battery or supercapacitor storage systems in Khorfakkan, United Arab Emirates. International Journal of Hydrogen Energy, 46 (8), 6014–6027, 2021. https://doi.org/10.1016/j.ijhydene.2020.08.153.
[31] C. Li, Y. Zeng, Z. Li, L. Zhang, L. Zhang, Y. Shan and Q. Tang, Techno-economic and environmental evaluation of grid-connected and off-grid hybrid intermittent power generation systems: A case study of a mild humid subtropical climate zone in China. Energy, 230, 1-16, 2021. https://doi.org/10.1016/j.energy.2021.120728.
[32] S.M. Tercan, A. Demirci, E. Gokalp and U. Cali, Maximizing self-consumption rates and power quality towards two-stage evaluation for solar energy and shared energy storage empowered microgrids. Journal of Energy Storage, 51, 1-13, 2022. https://doi.org/10.1016/j.est.2022.104561.
[33] A. Demirci, O. Akar and Z. Ozturk, Technical-environmental-economic evaluation of biomass-based hybrid power system with energy storage for rural electrification. Renewable Energy, 195, 1202–1217, 2022. https://doi.org/10.1016/j.renene.2022.06.097.
[34] Trading Economics, Inflation Rate. https://tradingeconomics.com/country-list/inflation-rate?continent=world (accessed Feb. 03, 2022).
[35] O. Ekren, C.H. Canbaz and Ç.B. Güvel, Sizing of a solar-wind hybrid electric vehicle charging station by using HOMER software. Journal of Cleaner Production, 279, 1-13, 2021. https://doi.org/10.1016/j.jclepro.2020.123615.

Appendix

COE (1): 14.0% IR, 23.31% DR, **COE (2):** 7.4% IR, 8.49% DR, **COE (3):** 1.3% IR, 4.3% DR.
(*) Optimal HPS

Table A.1. Morning Peak (With GSC)

PV (kW)	SCR (%)	SSR (%)	EE (%)	COE ($/kWh)		
				COE (1)	*COE (2)*	*COE (3)*
0	100.0	0.00	0.00	0.106	0.106	0.106
120	97.0	18.0	0.54	0.092	0.097	0.099
240 (*)	79.0	30.0	7.10	0.084	0.094	0.098
300	71.0	33.0	11.9	0.082	0.095	0.098
360	64.0	36.0	16.8	0.081	0.096	0.100
420	58.0	38.0	21.5	0.079	0.097	0.103
480	53.0	40.0	25.9	0.079	0.099	0.105
540	49.0	42.0	29.9	0.079	0.102	0.108
600 (*)	45.0	43.0	33.6	0.080	0.104	0.111
660	43.0	44.0	37.0	0.080	0.107	0.115
720	40.0	45.0	40.2	0.081	0.109	0.118
780	38.0	46.0	45.9	0.082	0.112	0.122
840	36.0	47.0	46.7	0.083	0.115	0.125
900	34.0	48.0	47.5	0.084	0.118	0.129

Table A.2. Midday Peak (With GSC)

PV (kW)	SCR (%)	SSR (%)	EE (%)	COE ($/kWh)		
				COE (1)	*COE (2)*	*COE (3)*
0	100.0	0.0	0.00	0.106	0.106	0.106
120	100.0	19.0	0.04	0.092	0.096	0.097
240	94.0	36.0	2.13	0.084	0.088	0.092
300 (*)	87.0	41.0	5.67	0.082	0.087	0.091
360	79.0	45.0	10.40	0.081	0.087	0.092
420	58.0	38.0	15.40	0.080	0.088	0.094
480	53.0	40.0	20.40	0.080	0.090	0.096
540 (*)	49.0	42.0	25.00	0.080	0.092	0.099
600	45.0	43.0	29.30	0.080	0.095	0.102
660	43.0	44.0	33.20	0.080	0.097	0.105
720	40.0	45.0	36.70	0.081	0.100	0.109
780	45.0	55.0	39.90	0.082	0.103	0.112
840	42.0	56.0	42.90	0.083	0.106	0.116
900	40.0	57.0	45.60	0.084	0.109	0.120

Table A.3. Evening Peak (With GSC)

PV (kW)	SCR (%)	SSR (%)	EE (%)	COE ($/kWh)		
				COE (1)	*COE (2)*	*COE (3)*
0	100.0	0.0	0.00	0.106	0.106	0.106
120 (*)	90.0	17.0	1.87	0.098	0.103	0.105
240	68.0	26.0	10.50	0.092	0.092	0.106
300	60.0	29.0	15.60	0.091	0.087	0.108
360	54.0	31.0	20.40	0.090	0.081	0.110
420 (*)	58.0	38.0	25.00	0.090	0.077	0.113
480	53.0	40.0	29.10	0.090	0.074	0.115
540	49.0	42.0	32.90	0.090	0.072	0.119
600	45.0	43.0	36.50	0.091	0.071	0.122
660	43.0	44.0	39.70	0.092	0.071	0.125
720	40.0	45.0	42.60	0.092	0.071	0.129
780	32.0	39.0	45.30	0.093	0.071	0.133
840	30.0	40.0	47.80	0.094	0.072	0.136
900	28.0	40.0	50.10	0.095	0.073	0.140

Table A.4. Morning Peak (Without GSC)

PV (kW)	SCR (%)	SSR (%)	EE (%)	COE ($/kWh)		
				COE (1)	*COE (2)*	*COE (3)*
0	100.0	0.0	0.00	0.106	0.106	0.106
120	97.0	18.0	0.00	0.091	0.097	0.099
240	79.0	30.0	0.00	0.075	0.086	0.089
300	71.0	33.0	0.00	0.067	0.080	0.084
360	64.0	36.0	0.00	0.060	0.075	0.079
420	57.0	38.0	0.00	0.053	0.070	0.075
480 (*)	53.0	40.0	0.00	0.047	0.065	0.071

540	48.0	42.0	0.00	0.042	0.061	0.067
600	43.0	44.0	0.00	0.038	0.058	0.064
660	42.5	44.0	0.00	0.034	0.054	0.061
720	39.8	45.0	0.00	0.030	0.051	0.058
780	37.5	46.0	0.00	0.027	0.049	0.055
840	35.5	47.0	0.00	0.024	0.046	0.053
900 (*)	33.7	48.0	0.00	0.021	0.044	0.051

Table A.5. Midday Peak (Without GSC)

PV (kW)	SCR (%)	SSR (%)	EE (%)	COE ($/kWh)		
				COE (1)	*COE (2)*	*COE (3)*
0	100.0	0.0	0.0	0.106	0.106	0.106
120	100.0	19.0	0.0	0.090	0.096	0.097
240	94.0	36.0	0.0	0.074	0.086	0.089
300	87.0	41.0	0.0	0.067	0.081	0.085
360	79.0	45.0	0.0	0.059	0.075	0.080
420	71.0	47.0	0.0	0.052	0.070	0.075
480 (*)	65.0	49.0	0.0	0.046	0.065	0.071
540	60.0	51.0	0.0	0.041	0.061	0.067
600	55.0	52.0	0.0	0.036	0.057	0.065
660	51.0	53.0	0.0	0.032	0.054	0.063
720	48.0	54.0	0.0	0.028	0.051	0.062
780	45.0	55.0	0.0	0.025	0.048	0.062
840	42.0	56.0	0.0	0.022	0.045	0.062
900 (*)	40.0	57.0	0.0	0.019	0.043	0.062

Table A.6. Evening Peak (Without GSC)

PV (kW)	SCR (%)	SSR (%)	EE (%)	COE ($/kWh)		
				COE (1)	*COE (2)*	*COE (3)*
0	100.0	0.0	0.00	0.106	0.106	0.106
120	90.0	17.0	0.02	0.095	0.101	0.103
240	68.0	26.0	0.07	0.078	0.089	0.092
300	60.0	29.0	0.11	0.070	0.083	0.087
360	54.0	31.0	0.36	0.063	0.077	0.081
420 (*)	49.0	32.0	1.04	0.056	0.072	0.077
480	45.0	34.0	2.55	0.051	0.068	0.073
540	41.0	35.0	4.60	0.046	0.064	0.069
600	38.0	36.0	6.97	0.041	0.060	0.066
660	36.0	37.0	9.63	0.037	0.057	0.063
720	34.0	38.0	12.3	0.033	0.054	0.060
780	32.0	39.0	15.0	0.030	0.051	0.058
840	30.0	40.0	17.5	0.027	0.049	0.055
900 (*)	28.0	40.0	20.1	0.024	0.047	0.053